HHS Public Access

Author manuscript

Cytokine Growth Factor Rev. Author manuscript; available in PMC 2020 November 01.

Published in final edited form as:

Cytokine Growth Factor Rev. 2019 October ; 49: 23–31. doi:10.1016/j.cytogfr.2019.10.004.

The transition model of RTK activation: a quantitative framework for understanding RTK signaling and RTK modulator activity

Michael D. Paul, **Kalina Hristova**

Department of Materials Science and Engineering, Institute for NanoBioTechnology, and Program in Molecular Biophysics , Johns Hopkins University, Baltimore MD 21218

Abstract

Here, we discuss the transition model of receptor tyrosine kinase (RTK) activation, which is derived from biophysical investigations of RTK interactions and signaling. The model postulates that (1) RTKs can interact laterally to form dimers even in the absence of ligand, (2) different unliganded RTK dimers have different stabilities, (3) ligand binding stabilizes the RTK dimers, and (4) ligand binding causes structural changes in the RTK dimer. The model is grounded in the principles of physical chemistry and provides a framework to understand RTK activity and to make predictions in quantitative terms. It can guide basic research aimed at uncovering the mechanism of RTK activation and, in the long run, can empower the search for modulators of RTK function.

Introduction

RTKs are the second largest family of membrane receptors [4]. They signal via lateral dimerization in the membrane to control cell growth, differentiation, and motility. Their dysregulation has been linked to many human diseases and disorders, including a variety of cancers [5–8]. There are 58 different RTKs in humans, grouped in 20 subfamilies, which all share the same basic architecture: an N-terminal extracellular (EC) region, a single-pass transmembrane (TM) domain, and an intracellular (IC) region containing a tyrosine kinase domain [9]. The RTK ligands, known as “growth factors,” are small, globular proteins, and are either monomers or constitutive dimers. They bind to the RTK’s EC region, and ultimately activate the kinases via a process that involves cross-phosphorylation on specific tyrosine residues. The activated kinases then phosphorylate additional tyrosines that serve as docking sites for adaptor proteins. The adaptors, in turn, bind cytoplasmic substrates and trigger downstream signaling pathways[5,9,11–14] such as MAPK, PI3K, PKC, and STAT.

This is an introduction to the transition model of RTK activation, which views RTK activation through the lens of physical chemistry (see Figure 1). The model states that (1)

Conflicts of interest

The authors declare no conflicts of interest.

RTKs have a propensity to interact laterally and to form dimers even in the absence of ligand, (2) different unliganded RTK dimers have different stabilities (and thus different dimer abundances at physiological concentrations), (3) ligand binding leads to RTK dimer stabilization, and (4) ligand binding induces structural changes in the RTK dimer. Thus, an increase in the expression level of the RTKs causes a transition from predominantly monomeric to predominantly dimeric populations, even in the absence of ligand. When ligand binds to the unliganded dimer, it induces a transition to a structurally distinct dimeric state with higher stability. We discuss experimental findings on which the model is based, and we identify missing basic knowledge that limits the utility of the model. We also demonstrate how the model can be used to understand and predict the action of RTK modulators.

(1) RTKs have a propensity to interact laterally and to form dimers even in the absence of ligand

Many of the biological responses that are mediated by RTKs occur specifically in response to ligands. It is now well established that ligand addition to cell cultures expressing RTKs induces RTK phosphorylation and downstream signaling, which leads to functional responses such as differentiation, migration, and contraction [13,15]. In the absence of ligand, often only low levels of phosphorylation—known as “basal phosphorylation”—are observed, and the functional responses are generally not seen [16]. Such observations were the basis for the first mechanistic model of RTK activation (the canonical model, Figure 1 Top), which postulates that the RTKs are monomeric in the absence of ligand, and the ligands crosslink them into dimers or higher order oligomers [7]. In this model, the ligand brings the kinase domains of two RTKs in close proximity, which enables the kinases to phosphorylate and activate each other.

However, experiments specifically designed to probe the association state of the receptors (rather than their phosphorylation status) have since revealed the presence of dimers or higher order oligomers in the plasma membrane of live cells in the absence of ligand. Unliganded dimers have been observed for many RTKs, including EGFR and other ErbBs, FGFRs, VEGFRs, and Trks, using a variety of techniques such as FRET, single-molecule tracking, FCS, and Number and Brightness [17,20–24]. It is thus clear that the ligand, while usually needed for RTK activation, is not necessarily needed for RTK dimerization/oligomerization. These findings have led to the concept that “RTK association is not enough,” as there are additional requirements for RTK activation to occur within the dimers [6,25–28].

The presence of unliganded RTK dimers appears significant in physiological context, even if they generally exhibit low or no activity. It is possible that unliganded dimerization potentiates the response of the receptor to ligand [11]. In particular, when unliganded dimers are present, the response to the ligand is not limited by the diffusion of the receptors in the plasma membrane and can be expected to be faster and more robust. Furthermore, unliganded dimers can be viewed as intermediates in the assembly of the fully active liganded dimers [29].

Many unliganded RTK dimers appear to be at least partially phosphorylated. This basal phosphorylation can have significant physiological consequences. For instance, increased unliganded dimerization and phosphorylation due to RTK overexpression has been linked to many cancers [30–33]. Targeting these unliganded dimers has proven to be a successful route for drug development [34–37]. Perhaps the best-known example is Herceptin, an antibody to the extracellular domain of ErbB2 (a receptor with no known ligand which is overexpressed in breast cancer). Indeed, herceptin has been shown to be an effective treatment in 30% of the ErbB2-positive metastatic breast cancer cases.

In addition to cancer, growth disorders can be caused by specific RTK mutations which increase unliganded dimerization[38,39]. One example is the G380R mutation in FGFR3, which causes the most common form of human dwarfism, achondroplasia [40,41]. This mutation increases ligand-independent FGFR3 dimerization and phosphorylation, without having a significant effect on FGFR3 phosphorylation in the presence of ligand[42,43].

For most RTKs, enhanced dimerization in the absence of ligand is pathogenic[35,44,45]. However, there are counterexamples, such as the case of EphA2. It has been shown that EphA2's pro-tumorigenic activity is mediated predominantly by the EphA2 monomer, and that EphA2 unliganded dimerization is anti-tumorigenic[1,46–48]. Accordingly, better understanding of the physical principles behind RTK dimerization may one day lead to novel anti-cancer therapies that either stabilize or disrupt the unliganded RTK dimers.

(2) Different unliganded RTK dimers have different stabilities (and thus different dimer abundance at physiological concentrations)

To evaluate the abundance of the unliganded dimers in the cell membrane, we must first quantify their association constants (and thus their dimer stabilities) using the tools of physical chemistry. Unliganded dimerization of RTKs in the plasma membrane can be described via the simple reaction scheme[49,50]:

$$M + M \overset{K}{\leftrightarrow} D$$

Here, M denotes the RTK monomers, and D denotes the RTK dimers. The constant K is the equilibrium dimerization constant defined as:

$$K = \frac{[D]}{[M]^2}$$

Often, the dissociation constant is used instead, given by the reciprocal value:

$$K_{diss} = \frac{1}{K} = \frac{[M]^2}{[D]}$$

Note that the plasma membrane is best viewed as a two-dimensional milieu, and hence the concentrations [M] and [D] are two-dimensional concentrations of monomers and dimers,

typically given in units of receptors per micron squared. Thus, the units for K are μm^2/rec, while the units for K_{diss} are rec/μm^2. The stability of the RTK dimer is defined as

$$\Delta G = -RT\ln\left(K/K_{st}\right).$$

with respect to a standard free energy $\Delta G_{st} = -RT\ln(K_{st})$. A common choice of reference state is K_{st} =1 nm^2/rec[49]. Therefore, if K_{diss} is reported in rec/μm^2, the stability of the dimer with respect to this standard state can be calculated as:

$$\Delta G = -RT\ln(K * 10^6) = RT\ln\left(K_{diss}/10^6\right)$$

To determine K_{diss} and ΔG, dimerization is quantified over a broad range of concentration by acquiring a dimerization curve, as done routinely with soluble proteins (for instance, as in the case of ligand binding to a soluble protein)[51]. Such data can then be fit to a dimer model to calculate K_{diss} and the dimer stabilities, and to evaluate if a dimerization model can describe the data [52].

Using a FRET-based approach, we have quantified the dimerization of several RTKs in the plasma membrane of mammalian cells. The dissociation constants have been found to vary between 12±2 rec/μm^2 (for TrkB) to 710 ± 100 rec/μm^2 (for FGFR1) [1,2,17,22,29]. The dimerization curves (dimeric fraction versus receptor concentration) for all studied receptors are compared in Figure 2.

In Figure 2, we see that the different dimeric fractions at a specific receptor concentration, such as 100 rec/μm^2, vary significantly. FGFR1 has the lowest dimeric fraction, as only about 30% of the FGFR1 molecules exist as dimers at this concentration. Since FGFR1 is predominantly monomeric under these conditions, it may be incorrectly categorized as following the canonical model of RTK activation, especially if the experimental technique used lacks quantitative power. In contrast, 80% of the TrkB molecules are dimeric at the chosen concentration of 100 rec/μm^2, which may lead to the incorrect conclusion that the behavior of TrkB is fundamentally different from the behavior of FGFR1. Indeed, TrkB has been referred to as a “pre-formed dimer” in the literature [23]. Yet, the only difference is in the exact value of the dimerization constant—both receptors follow the transition model of RTK activation.

Figure 2 helps us appreciate that both the expression level and the dissociation constants dictate RTK dimerization levels. Note that an increase in FGFR1 concentration from 100 to 1,000 rec/μm^2 (as occurs in overexpression in cancer) increases the dimeric population from 30% to 50%. For TrkB at the physiological expression of 20 rec/μm^2, about 60% of the receptors are dimeric. As a rule, high populations of dimers are expected when the expression is higher than the dissociation constant, while low dimer populations are expected when the expression is lower than the dissociation constant.

RTK expression levels vary during development and in disease [53–57]. However, exact expression levels are rarely measured and are largely unknown, limiting our understanding

of RTK behavior in different cellular contexts. We are looking forward to new quantitative measurements of expression levels that will help us understand how cells fine-tune RTK function by modulating their expression.

(3) Ligand binding leads to RTK dimer stabilization

While now it is clear that ligands are not required for RTK dimerization, they are widely believed to stabilize the RTK dimers upon binding to their EC domains. For years, this view was shaped by crystal structures of isolated soluble EC domains which either show stabilizing interactions between ligands and the two receptors, or ligand-induced rearrangements in the RTK EC domains, leading to the induction of dimerization interfaces and stabilizing contacts between the two chains [58–64]. However, direct measurements of RTK dimer stabilization are rare and are not in agreement.

For RTKs, ligand binding is coupled to RTK dimerization [3,65]. This coupling can easily be understood though the use of thermodynamic cycles, such as those shown in Figure 3. Such cycles provide the best description of the transition model, as they show how increases in both receptor and ligand concentration drive the transition to active liganded RTK dimers via intermediate states.

The case of dimeric RTK ligands

The cycle in Figure 3A describes the activation of an RTK dimer by dimeric ligand. An example of this process is the activation of VEGFR2 by its constitutively dimeric (disulfide-linked) ligand, VEGF. The dimerization constants in the cycles are denoted as K's, and the ligand-binding constants are denoted as L's. The Y constants denote possible allosteric transitions in the dimers. Figure 3C defines the association constants, and Figure 3E shows the links between these association constants. As expected from allosteric theory, the conformational change is invisible in binding experiments [66], and thus the true binding and transition constants cannot be decoupled from each other. Therefore, the cycle in Figure 4A is the working model that can be used in binding/dimerization data fitting. As predicted by the allosteric interaction theory [66], the dimers bind ligands with apparent affinities, "Λ's," equal to the product of the binding and allosteric transition constants. Similarly, liganded monomers form activated, liganded dimers with apparent dimerization constants, "κ's," equal to the product of the dimerization and allosteric transition constants.

The case of monomeric ligands

The cycle in Figure 3B shows the binding of two monomeric ligands to an RTK dimer. An example of this is the binding of the monomeric EGF ligands to the EGFR dimer, under the assumption that EGFR can form only dimers and no higher order oligomers (questioned recently, see the section on RTK oligomerization below). Figure 3D shows the definitions of the association constants, and Figure 3F reports the links between these association constants. In Figure 4B, we show the working model that can be used in binding/dimerization data fitting for a monomeric ligand.

Direct quantification of dimer stabilization due to ligand.

Dimer stabilization can be quantified by comparing the association constant $\kappa 2$ in the dimeric ligand cycle (or both $\kappa 2$ and $\kappa 3$ in the monomeric ligand cycle) to $K1$. For instance, if $\kappa 2$ is greater than $K1$, then the ligand has a stabilizing effect, with a larger difference corresponding to a larger stabilization.

Direct measurements of RTK dimer stabilities can be performed in the presence of a known ligand concentration using FRET [49,50,67,68] or coimmunoimmobilization assay (co-II) [69], similarly to the case of no ligand. This requires quantification of dimer fraction as a function of receptor expression and ligand concentration, such that all the data can be fit to the appropriate thermodynamic cycle (as in Figure 4). To understand the behavior of the receptors in the presence of monomeric and dimeric ligands, we modeled the abundance of the liganded, active dimers and other receptor states. Figure 5 shows the total predicted liganded dimeric fractions for different ligand concentrations in the cases of dimeric and monomeric ligands. These predications are based on experimentally determined dimer and ligand-binding constants [29,65,68]. We see very different behaviors in the two cases: in the case of dimeric ligand (Figure 5, top), liganded dimeric fraction increases and then decreases as the ligand concentration is increased, while in the case of monomeric ligand (Figure 5, bottom), the liganded dimeric fraction monotonically increases with ligand concentration and comes to saturation. The fact that increasing concentrations of dimeric ligand can cause the liganded dimeric fraction to decrease is rarely taken to accounts and warrants emphasis. Ligand experiments are sometimes performed under “saturating” conditions of ligand, but no such state exists for a dimeric ligand, and using too high concentrations of dimeric ligand can result in a significant underestimation of interactions and functional outputs.

In the case of dimeric ligand, this behavior is a consequence of the fact that one ligand has two binding sites for the receptor. This means that only one ligand is bound to a dimer of receptors. Accordingly, the dimerization constant $K3$ (or $\kappa 3$) (Figures 3A and 4A) depends on the ligand concentration, as it describes the interaction of two liganded monomers forming one liganded dimer and releasing a ligand into solution. At high ligand concentrations, receptors effectively become trapped as liganded monomers, and hence the dimeric fraction decreases. It is therefore important that measurements of $K3$ in the case of dimeric ligand always specify the exact ligand concentration. For example, we have reported that the contributions of the three neurotrophin ligands to Trk dimer stability varies from approximately −1.5 to −2.5 kcal/mole, at 380 nM ligand[17]. Following the prediction in Figure 5, top, we expect that the stabilization effect of the ligand will be reduced when the concentration of the dimeric neurotrophin ligands is further increased. In the case of EGFR and its monomeric ligand, EGF, we have reported that the EGF dimer is stabilized by −3.0 kcal/mole in the presence of 780 nM EGF[70]. This value should not change significantly as the concentration of ligand is increased (see Figure 5, bottom).

Measurements of molecular ligand binding constants report on ligand-induced dimer stabilization

In cases where $K1$ and $\kappa 2$ are not measured directly, the stabilization effect of the ligand can be assessed through measurements of ligand binding constants to both RTK monomers and

RTK dimers. This is possible because the stabilization effect, quantified through the ratio of the dimerization constants in the presence and absence of ligand, is equal to the ratio of the ligand binding constants (see Figures 3E and 3F).

In a recent example, we quantified the binding of VEGF to VEGFR2 by directly measuring $L1$ and $\Lambda 2$ [65]. These experiments entailed measurements of the surface densities of fluorescently-labeled VEGFR2 and VEGF, as well as the free VEGF concentration in twelve independent experiments at different free-ligand concentrations varying over two orders of magnitude, from 0.21 nM to 42.4 nM. The data were interpreted with the thermodynamic cycle in Figure 4A. A global fit was performed to find the optimal values of the binding affinity of VEGF for monomeric VEGFR2, $L1$, and the binding affinity of VEGF for dimeric VEGFR2, $\Lambda 2$. The dissociation constants were determined to be 10 nM for $L1$ and 230 pM for $\Lambda 2$. Thus, there is a 45-fold enhancement of VEGF binding to dimeric VEGFR2 over binding to monomeric VEGFR2. Since ligand binding and dimerization are coupled, this means that $\kappa 2$ is also 45 times greater than $K1$, which is a significant stabilization effect.

In another example, Macdonald and Pike measured EGF binding to EGFR and fit the binding data to the cycle shown in Figure 4B [71]. They measured binding of radiolabeled EGF to cell monolayers that were stably transfected with a plasmid that encoded for EGFR under the control of a tet-inducible promoter, thus varying both the EGF concentration and the EGFR expression. The dissociation constant of unliganded dimerization was determined to be ~110 rec/μm^2, and that for one unliganded EGFR with one liganded EGFR as ~130 rec/μm^2. On the other hand, the dissociation constant describing the lateral dimerization of two liganded EGFRs was determined to be ~1300 rec/μm^2, indicating that the bound ligand destabilizes the EGFR dimer. These measurements, however, do not agree with the direct measurements of EGFR dimer stability in the presence of ligand. Both FRET and the recently developed Co-II—which is based on single molecule particle tracking—show that the EGFR dimer is stabilized in the presence of EGF [69,70]. This means that the dimeric fraction increases with increasing concentration of ligand, while the values measured by Macdonald and Pike predict that the dimeric fraction decreases with increasing ligand concentration until it reaches a plateau with a value determined by $\kappa 3$. A possible explanation for this discrepancy is that EGFR can form oligomers [72,73], and hence the cycle in Figure 3B/4B does not apply (see below). Thus, more work is needed before we can draw definitive conclusions about the role of EGF in modulating EGFR dimer stability. Furthermore, the effect of ligands on RTK dimer stability still remains to be investigated for most of the 58 RTKs.

Can dimer stability be predicted based on crystal structure or effective binding constants?

It is tempting to inspect crystal structures of ligand-bound, isolated RTK EC domains and speculate about the extent of dimer stabilization by a ligand. However, predicting the effects of a ligand on RTK dimer stability requires us to consider ligand binding to both monomers and dimers. Thus, the structure of the ligand-bound dimers is not sufficient for stability predictions.

It is further worth noting that ligand binding measurements to both RTK monomers and RTK dimers (i.e., measurements of molecular binding constants) are rare in the literature, as

typically experiments quantify only the effective ligand binding constants, which do not take into account the effects of receptor concentration and receptor association state. The effective dissociation constant is defined as

$$Keff = \frac{[\mathrm{L}][\text{free RTK}]}{[\text{bound RTK}]},$$

and is determined from a binding isotherm,

$$\mathrm{f} = \frac{[\mathrm{L}]}{[\mathrm{L}] + Keff}.$$

$Keff = \frac{[\mathrm{L}]([\mathrm{M}] + 2[\mathrm{D}])}{([\mathrm{ML}] + 2[\mathrm{DL}])}$,, and thus *Keff* depends on the molecular binding constants in Figures 3 and 4, but they cannot be extracted from such measurements. Accordingly, literature values of ligand-receptor dissociation constants vary widely, because receptor concentrations are variable in the different experiments[59,74–76]. The effective binding constants are inherently different in different experimental contexts, due to differences in the association state of the receptors in the different contexts. We are therefore looking forward to the development of novel approaches that quantify molecular ligand binding constants and ultimately report on the effect of ligand on dimer stability. We believe that the fluorescence-based method that we have used to quantify VEGF binding [65], described above, is an important step towards this goal.

Can ligand cause oligomerization?

It has long been known that the receptors of the Eph family form clusters in response to their ligands, and that clustering is critically important for their biological activity [8,77,78]. Lately, it has been suggested that EGFR can also oligomerize in response to EGF, in a manner that is dependent on EGF concentration [72,73,79]. Specifically, oligomerization has been proposed to occur at low EGF concentration, as it is mediated by ligand-binding sites that are not occupied by ligand [72]. Furthermore, it has been proposed that EGFR activation is optimal in the oligomers and not the dimers, with phosphorylation occurring in a cooperative manner between neighboring dimers. However, the extent of EGFR oligomerization is still debated in the literature, and this model is not universally accepted [69]. If EGFR oligomerization indeed occurs and depends on the ligand concentration, it should be included in thermodynamic cycles such as the ones in Figure 3A and 4A. As pointed out above, the disagreement about the extent of ligand-induced EGFR stabilization in different studies may be due to the fact that the thermodynamic cycle in Figure 3B/4B does not adequately describe EGFR, as it does not take oligomereization into account. It remains to be seen if oligomerization is important for other RTKs; further research is needed to address this issue.

(4) Ligand binding induces structural changes in the RTK dimers

It is widely believed that mechanisms exist that prevent the spontaneous activation of unliganded RTK dimers [14]. For instance, the ligand likely induces structural changes that are required for robust kinase activation and downstream signaling [22,26,29,80,81]. An intuitive

mechanism is that structural changes are initiated in the EC domain in response to ligand binding and are propagated along the length of the RTK. This is presumably facilitated by a "hard" linkage between the domains that allows for the transmission of structural information along the length of the RTK [82]. Such allosteric structural changes are incorporated into the transition model in Figure 3 through the Y constants. As discussed above, these constants cannot be directly measured in dose-response binding experiments, as the structural transition is tightly coupled to the binding interactions. Based on the current understanding of RTK activation, it can be assumed that $Y1$ is small (assuming that the unliganded dimers are not likely to adopt an active conformation), while $Y2$ and $Y3$ are large (assuming that the ligand-bound dimers have a strong preference for the activated conformation). Note that the transition model naturally incorporates the possibility of ligand bias (i.e., the fact that different ligands can stabilize different receptor configurations) as the values of Y may be different for each ligand.

The extent of structural coupling between the different RTK domains is under debate; some believe that the linkage between the domains is flexible, and hence structural changes from the EC domain cannot be transmitted to the kinase domain [83]. Evidence for this view is that one ligand-bound EGFR EC domain state can correspond to multiple kinase domain conformations [84], and that one EGFR kinase state can correspond to multiple EC domain states [85]. There are limited studies addressing this issue, as most of the biophysical and structural work has been done with isolated domains, not full-length RTKs.

There are no full-length RTK dimer structures, for any of the RTKs, and we have limited knowledge about the mechanism of signal propagation along the length of the RTKs. Accordingly, approaches that can be used to monitor the intracellular (IC) domains in cells are very useful, as they can shed light on the response of the IC region to ligand binding. One possible read-out is the FRET efficiency between the intracellularly attached fluorophores, which can be measured both in the absence and presence of ligand [86]. In the case where the RTKs are 100% dimers, differences in FRET efficiency are caused by differences in the relative positioning and dynamics of the phosphorylated dimers [17,22,29,87]. Under conditions where the receptors instead explore a monomer-dimer equilibrium, this information can be obtained by fitting the FRET data to a dimerization model to decouple the contributions of dimer stabilization and conformational changes to the change in the FRET signal [67]. Another possibility is to use single-molecule techniques which have the resolution to determine small changes in distance and conformation upon addition of ligand [88–90].

The FRET-based approach has revealed changes in the relative positioning and dynamics of fluorescent proteins when they are attached intracellularly to the TM domain C-termini [17,22,29]. These findings support a long-standing idea in the literature that the TM domains can interact through multiple interfaces and dimerization motifs, and that the ligand induces a switch from one conformation to another [6,25,81,91–94]. This change in TM conformation may lead to a change in the position of the kinase domains (if the kinase and TM domains are structurally linked) or could contribute to the overall stabilization of the dimer.

Differences in FRET have also been observed in experiments where the fluorescent proteins are attached to the C-termini of the full-length RTKs [17]. Generally, such experiments are more difficult to interpret, because the kinase domains and the flexible C-terminal tails can adopt many more configurations than the simple TM helices in the bilayer [95]. It is possible that the kinases explore different conformations both in the absence and presence of ligand, and that their interactions are highly dynamic, giving rise to FRET efficiencies that are averaged over many configurations. In this case, the effect of the ligand may be to alter the dynamics of the kinases and to cause shifts in the relative time spent in the different configurations. Therefore, new experimental approaches, perhaps based on single molecule detection or NMR, are needed to elucidate the response of the kinases to the bound ligand.

It is important to note that possible structural changes in the kinase domain can be facilitated by other proteins. In the case of FGFR2, it has been suggested that dimeric Grb2 binds to the C-termini of the two FGFR2 molecules in an unliganded dimer [11]. In this state, the FGFR2 unliganded dimer exhibits a low level of phosphorylation, and the recruitment of downstream adaptor proteins is prevented. Upon ligand binding, FGFR2 phosphorylates Grb2, prompting Grb2 to dissociate and to allow downstream signaling. It is not clear if this mechanism is a common occurrence in RTK signaling, or if it is an isolated case that only applies to FGFR2. Regardless, it is an excellent illustration of the fact that other cellular proteins may be playing important roles in RTK activation, and they need to be considered as we develop new approaches to study RTK signaling.

Utility of the transition model: Predicting the effects of RTK modulators

The transition model can help us understand the action of different pharmacological modulators, once their binding properties are known. In particular, the transition model can directly account for the action of the modulator by expanding the thermodynamic cycles in Figures 3 and 4 to incorporate the interactions of the modulator with the receptor and the ligand as needed. Examples are shown in Figures 6A and B. The thermodynamic cycle in Figure 6A describes the action of an inhibitor which blocks receptor dimerization, but does not directly interfere with the binding of a dimeric ligand to the receptor. In particular, this inhibitor is assumed to bind to unliganded monomers (M) and liganded monomer (ML) only. On the other hand, Figure 6B describes an inhibitor which competes with ligand binding, but does not directly interfere with dimerization. This inhibitor is assumed to bind to unliganded monomers (M) and unliganded dimers (D) only.

Figures 6C and D show the predictions for the effect of these two different RTK inhibitors on the total liganded RTK dimeric fraction. These predictions are based on measured binding and dimerization constants for VEGF-VEGFR2 [65], but arbitrarily chosen binding constants for the two inhibitors (see Figure 6 legend for exact values). The black curve is the case of no inhibitor. The blue curve corresponds to the case in Figure 6A: an inhibitor which blocks dimerization, but does not directly interfere with ligand binding. The red curve corresponds to the case in Figure 6B: an inhibitor which competes with ligand binding, but does not directly interfere with dimerization. Figure 6C shows the liganded dimeric fraction (i.e., the fraction of receptors in the active state) as a function of inhibitor concentration, where the ligand concentration is 1 nM—a VEGF concentration that is commonly used in

cell culture experiments. Figure 6D is the liganded dimeric fraction as a function of ligand concentration, where the inhibitor concentration is fixed at 1 nM. As seen by the different shapes of the curves, the two inhibitors have different effects. At 1 nM ligand concentration (dashed magenta line), and for the chosen binding constants, the inhibitory effect of the ligand binding inhibitor is predicted to be greater than the effect of the dimerization inhibitor. However, as the concentration of ligand increases, the dimerization inhibitor becomes more potent than the ligand-binding inhibitor. This demonstrates the utility of the transition model, as the effects of the different inhibitors are difficult to predict without quantitative modeling. Of note, the effect of the inhibitor is strongly dependent on its binding strength relative to the ligand: inhibitors with much weaker binding will have little effect and inhibitors with much stronger binding can completely abolish the presence of liganded dimers.

Conclusion

The transition model of RTK activation, discussed here, is derived from biophysical studies of several RTK subfamilies. This testable model can be used as a guideline for better understanding of the mechanism of RTK activation. The model enables predictions of liganded dimer populations, and thus predictions of RTK activity based on measurements of dimerization constants, ligand-binding constants, and expression levels of the RTKs and their ligands in different tissues.

Currently, it is not known how universal the transition model is, as the model has not yet been tested in the context of many RTKs. It is further not known if the transition model can explain all aspects of the activation of an RTK. A broader study of the applicability of the model across the different RTK subfamilies will uncover both the similarities and differences in the activation mechanism of the different RTKs. The identified common features will delineate the most fundamental physical-chemical principles that underlie RTK activity.

The utility of the transition model is currently limited by gaps in knowledge of molecular ligand binding constants, of the association state of the receptors as a function of ligand concentration, of expression levels of receptors and ligands in cells and tissues, and of the nature of conformational changes in the intracellular portion of the dimer that occur (or not) in response to ligand binding. The lack of knowledge is often due to limitations in experimental methodologies. We are confident that in the near future the scientific community will develop and implement new quantitative methodologies that report on receptor activation, full-length receptor structure, and receptor-ligand and receptor-receptor interactions. We believe that techniques that yield information about structure and dynamics in the context of the full-length receptors in live cells in response to ligand will be particularly useful. We have no doubt that our understanding of RTK signaling will continue to rapidly grow.

Finally, the transition model can help us determine the mode of action of an RTK modulator, by reporting on the physical processes that are most affected by it. Importantly, the various effects can be directly quantified by comparing binding constants with and without the

modulator. Such knowledge will empower the optimization of both RTK inhibitors and RTK activators, to be used as tools in basic scientific research or as therapeutics in the clinic.

Acknowledgements:

Supported by NSF MCB 1712740 and NIH GM068619.

Biographies

Michael D. Paul received B.S. degrees in chemistry, biochemistry, and mathematics from the University of Chicago in 2014. After graduating, he joined the Johns Hopkins Program in Molecular Biophysics for his Ph.D. His current research is focused on using quantitative florescence microscopy methods and thermodynamic modeling to understand protein-protein interactions in the plasma membrane of cells.

Kalina Hristova received her B.S. and M.S. degrees in Physics from the University of Sofia, Bulgaria, and her Ph.D. degree in Mechanical Engineering and Materials Science from Duke University, USA. She did post-doctoral work at the University of California, Irvine. She is now a Professor of Materials Science and Engineering at the Institute for NanoBioTechnology at Johns Hopkins University. Dr. Hristova is the recipient of the 2007 Margaret Oakley Dayhoff award from the Biophysical Society. She was elected Fellow of the American Physical Society in 2016, and Fellow of the American Institute for Medical and Biological Engineering in 2018. The main focus of the research in her laboratory is the physical principles that underlie membrane protein folding and signal transduction across biological membranes.

References

1. Singh DR, Kanvinde P, King C, Pasquale EB & Hristova K The EphA2 receptor is activated through induction of distinct, ligand-dependent oligomeric structures. Commun Biol 1, 15, (2018). [PubMed: 30271902]
2. Singh DR et al. Unliganded EphA3 dimerization promoted by the SAM domain. Biochemical Journal 471, 101–109 (2015). [PubMed: 26232493]
3. Paul MD & Hristova K The RTK Interactome: Overview and Perspective on RTK Heterointeractions. Chem Rev 119, 5881–5921, (2019). [PubMed: 30589534]
4. Fantl WJ, Johnson DE & Williams LT Signaling by Receptor Tyrosine Kinases. Annual Review of Biochemistry 62, 453–481 (1993).
5. Schlessinger J Cell signaling by receptor tyrosine kinases. Cell 103, 211–225 (2000). [PubMed: 11057895]
6. Li E & Hristova K Role of receptor tyrosine kinase transmembrane domains in cell signaling and human pathologies. Biochemistry 45, 6241–6251 (2006). [PubMed: 16700535]

7. Weiss A & Schlessinger J Switching signals on or off by receptor dimerization. Cell 94, 277–280 (1998). [PubMed: 9708728]
8. Pasquale EB Eph receptors and ephrins in cancer: bidirectional signalling and beyond. Nature Reviews Cancer 10, 165–180 (2010). [PubMed: 20179713]
9. Lemmon MA & Schlessinger J Cell Signaling by Receptor Tyrosine Kinases. Cell 141, 1117–1134 (2010). [PubMed: 20602996]
10. Sarabipour S & Hristova K Mechanism of FGF receptor dimerization and activation. Nat Commun 7, (2016).
11. Lin CC et al. Inhibition of Basal FGF Receptor Signaling by Dimeric Grb2. Cell 149, 1514–1524 (2012). [PubMed: 22726438]
12. Lemmon MA, Schlessinger J & Ferguson KM The EGFR family: not so prototypical receptor tyrosine kinases. Cold Spring Harbor perspectives in biology 6, a020768 (2014). [PubMed: 24691965]
13. Schlessinger J Receptor tyrosine kinases: legacy of the first two decades. Cold Spring Harbor perspectives in biology 6, a008912 (2014). [PubMed: 24591517]
14. Schlessinger J Autoinhibition control. Science 300, 750–752 (2003). [PubMed: 12730587]
15. Lemmon MA & Schlessinger J Cell signaling by receptor tyrosine kinases. Cell 141, 1117–1134, (2010). [PubMed: 20602996]
16. Liang SI et al. Phosphorylated EGFR Dimers Are Not Sufficient to Activate Ras. Cell Rep 22, 2593–2600, (2018). [PubMed: 29514089]
17. Ahmed F & Hristova K Dimerization of the Trk receptors in the plasma membrane: effects of their cognate ligands. Biochem J 475, 3669–3685 (2018). [PubMed: 30366959]
18. Schlessinger J Ligand-induced, receptor-mediated dimerization and activation of EGF receptor. Cell 110, 669–672 (2002). [PubMed: 12297041]
19. Sarabipour S, Ballmer-Hofer K & Hristova K VEGFR-2 conformational switch in response to ligand binding. Elife 5, e13876 (2016). [PubMed: 27052508]
20. Yu XC, Sharma KD, Takahashi T, Iwamoto R & Mekada E Ligand-independent dimer formation of epidermal growth factor receptor (EGFR) is a step separable from ligand-induced EGFR signaling. Molecular Biology of the Cell 13, 2547–2557 (2002). [PubMed: 12134089]
21. Tao RH & Maruyama IN All EGF(ErbB) receptors have preformed homo- and heterodimeric structures in living cells. Journal of Cell Science 121, 3207–3217 (2008). [PubMed: 18782861]
22. Sarabipour S & Hristova K Mechanism of FGF receptor dimerization and activation. Nat.Commun 7, 10262 (2016). [PubMed: 26725515]
23. Maruyama I & Shen JY Brain-derived neurotrophic factor receptor TrkB exists as a preformed dimer in living cells. FASEB Journal 26 (2012).
24. Nagy P, Claus J, Jovin TM & Arndt-Jovin DJ Distribution of resting and ligand-bound ErbB1 and ErbB2 receptor tyrosine kinases in living cells using number and brightness analysis. Proc.Natl.Acad.Sci.U.S.A 107, 16524–16529 (2010). [PubMed: 20813958]
25. Li E & Hristova K Receptor Tyrosine Kinase transmembrane domains: function, dimer structure, and dimerization energetics. Cell Adhesion and Migration 4, 249–254 (2010). [PubMed: 20168077]
26. Moriki T, Maruyama H & Maruyama IN Activation of preformed EGF receptor dimers by ligand-induced rotation of the transmembrane domain. Journal of Molecular Biology 311, 1011–1026 (2001). [PubMed: 11531336]
27. Yang Y, Xie P, Opatowsky Y & Schlessinger J Direct contacts between extracellular membrane-proximal domains are required for VEGF receptor activation and cell signaling. Proceedings of the National Academy of Sciences of the United States of America 107, 1906–1911 (2010). [PubMed: 20080685]
28. Hyde CA et al. Targeting extracellular domains D4 and D7 of vascular endothelial growth factor receptor 2 reveals allosteric receptor regulatory sites. Molecular and Cellular Biology 32, 3802–3813 (2012). [PubMed: 22801374]
29. Sarabipour S, Ballmer-Hofer K & Hristova K VEGFR-2 conformational switch in response to ligand binding. Elife 5 (2016).

30. Barker FG et al. EGFR overexpression and radiation response in glioblastoma multiforme. International Journal of Radiation Oncology Biology Physics 51, 410–418 (2001).
31. Kornmann M, Beger HG & Korc M Role of fibroblast growth factors and their receptors in pancreatic cancer and chronic pancreatitis. Pancreas 17, 169–175 (1998). [PubMed: 9700949]
32. Turner N et al. FGFR1 Amplification Drives Endocrine Therapy Resistance and Is a Therapeutic Target in Breast Cancer. Cancer Research 70, 2085–2094 (2010). [PubMed: 20179196]
33. Hafner C et al. Differential gene expression of Eph receptors and ephrins in benign human tissues and cancers. Clinical Chemistry 50, 490–499 (2004). [PubMed: 14726470]
34. Hynes NE & Lane HA ERBB receptors and cancer: The complexity of targeted inhibitors. Nature Reviews Cancer 5, 341–354 (2005). [PubMed: 15864276]
35. Browne BC, O'Brien N, Duffy MJ, Crown J & O'Donovan N HER-2 Signaling and Inhibition in Breast Cancer. Current Cancer Drug Targets 9, 419–438 (2009). [PubMed: 19442060]
36. Brunelleschi S, Penengo L, Santoro MM & Gaudino G Receptor tyrosine kinases as target for anti-cancer therapy. Current Pharmaceutical Design 8, 1959–1972 (2002). [PubMed: 12171522]
37. Ross JS et al. The HER-2 Receptor and Breast Cancer: Ten Years of Targeted Anti-HER-2 Therapy and Personalized Medicine. Oncologist 14, 320–368 (2009). [PubMed: 19346299]
38. Cohen MM Some chondrodysplasias with short limbs: Molecular perspectives. American Journal of Medical Genetics 112, 304–313 (2002). [PubMed: 12357475]
39. Wilkie AOM Bad bones, absent smell, selfish testes: The pleiotropic consequences of human FGF receptor mutations. Cytokine & Growth Factor Reviews 16, 187–203 (2005). [PubMed: 15863034]
40. Aviezer D, Golembo M & Yayon A Fibroblast growth factor receptor-3 as a therapeutic target for achondroplasia - Genetic short limbed dwarfism. Current Drug Targets 4, 353–365 (2003). [PubMed: 12816345]
41. Foldynova-Trantirkova S, Wilcox WR & Krejci P Sixteen Years and Counting: The Current Understanding of Fibroblast Growth Factor Receptor 3 (FGFR3) Signaling in Skeletal Dysplasias. Human Mutation 33, 29–41 (2012). [PubMed: 22045636]
42. He L, Horton WA & Hristova K The physical basis behind achondroplasia, the most common form of human dwarfism. Journal of Biological Chemistry 285 30103–30114 (2010). [PubMed: 20624921]
43. He L, Wimley WC & Hristova K FGFR3 heterodimerization in achondroplasia, the most common form of human dwarfism. Journal of Biological Chemistry 286 13272–13281 (2011). [PubMed: 21324899]
44. Collisson EA et al. Comprehensive molecular profiling of lung adenocarcinoma. Nature 513, 543–550 (2014). [PubMed: 25254475]
45. Marmor MD, Skaria KB & Yarden Y Signal transduction and oncogenesis by ErbB/HER receptors. International Journal of Radiation Oncology Biology Physics 58, 903–913 (2004).
46. Singh DR et al. EphA2 Receptor Unliganded Dimers Suppress EphA2 Pro-tumorigenic Signaling. Journal of Biological Chemistry 290, 27271–27279 (2015). [PubMed: 26363067]
47. Paraiso KH et al. Ligand-Independent EPHA2 Signaling Drives the Adoption of a Targeted Therapy-Mediated Metastatic Melanoma Phenotype. Cancer Discov. 5, 264–273 (2015). [PubMed: 25542447]
48. Miao H et al. EphA2 Mediates Ligand-Dependent Inhibition and Ligand-Independent Promotion of Cell Migration and Invasion via a Reciprocal Regulatory Loop with Akt. Cancer Cell 16, 9–20 (2009). [PubMed: 19573808]
49. Chen LR, Novicky L, Merzlyakov M, Hristov T & Hristova K Measuring the Energetics of Membrane Protein Dimerization in Mammalian Membranes. Journal of the American Chemical Society 132, 3628–3635 (2010). [PubMed: 20158179]
50. Sarabipour S, Del Piccolo N & Hristova K Characterization of Membrane Protein Interactions in Plasma Membrane Derived Vesicles with Quantitative Imaging Forster Resonance Energy Transfer. Acc.Chem.Res 48, 2262–2269 (2015). [PubMed: 26244699]
51. Sarabipour S, Del Piccolo N & Hristova K Characterization of membrane protein interactions in plasma membrane derived vesicles with quantitative imaging Forster resonance energy transfer. Acc Chem Res 48, 2262–2269 (2015). [PubMed: 26244699]

52. King C, Raicu V & Hristova K Understanding the FRET Signatures of Interacting Membrane Proteins. J Biol Chem 292, 5291–5310 (2017). [PubMed: 28188294]
53. Abbass SAA, Asa SL & Ezzat S Altered expression of fibroblast growth factor receptors in human pituitary adenomas. Journal of Clinical Endocrinology and Metabolism 82, 1160–1166 (1997). [PubMed: 9100589]
54. Day BW et al. EphA3 Maintains Tumorigenicity and Is a Therapeutic Target in Glioblastoma Multiforme. Cancer Cell 23, 238–248 (2013). [PubMed: 23410976]
55. Wagh PK, Peace BE & Waltz SE Met-related receptor tyrosine kinase Ron in tumor growth and metastasis. Adv.Cancer Res 100, 1–33 (2008). [PubMed: 18620091]
56. Cross MJ & Claesson-Welsh L FGF and VEGF function in angiogenesis: signalling pathways, biological responses and therapeutic inhibition. Trends in Pharmacological Sciences 22, 201–207 (2001). [PubMed: 11282421]
57. Smith NR et al. Vascular Endothelial Growth Factor Receptors VEGFR-2 and VEGFR-3 Are Localized Primarily to the Vasculature in Human Primary Solid Cancers. Clinical Cancer Research 16, 3548–3561 (2010). [PubMed: 20606037]
58. Plotnikov AN, Schlessinger J, Hubbard SR & Mohammadi M Structural basis for FGF receptor dimerization and activation. Cell 98, 641–650 (1999). [PubMed: 10490103]
59. Mohammadi M, Olsen SK & Ibrahimi OA Structural basis for fibroblast growth factor receptor activation. Cytokine & Growth Factor Reviews 16, 107–137 (2005). [PubMed: 15863029]
60. Goetz R & Mohammadi M Exploring mechanisms of FGF signalling through the lens of structural biology. Nat.Rev.Mol.Cell Biol 14, 166–180 (2013). [PubMed: 23403721]
61. Burgess AW et al. An open-and-shut case? Recent insights into the activation of EGF/ErbB receptors. Molecular Cell 12, 541–552 (2003). [PubMed: 14527402]
62. Cho HS & Leahy DJ Structure of the extracellular region of HER3 reveals an interdomain tether. Science 297, 1330–1333 (2002). [PubMed: 12154198]
63. Bouyain S, Longo PA, Li SQ, Ferguson KM & Leahy DJ The extracellular region of ErbB4 adopts a tethered conformation in the absence of ligand. Proceedings of the National Academy of Sciences of the United States of America 102, 15024–15029 (2005). [PubMed: 16203964]
64. Ferguson KM et al. EGF activates its receptor by removing interactions that autoinhibit ectodomain dimerization. Molecular Cell 11, 507–517 (2003). [PubMed: 12620237]
65. King C & Hristova K Direct measurements of VEGF-VEGFR2 binding affinities reveal the coupling between ligand binding and receptor dimerization. J Biol Chem 294, 9064–9075 (2019). [PubMed: 31023826]
66. Jackson MB Molecular and cellular biophysics (Cambridge University Press, 2006).
67. Chen L, Placone J, Novicky L & Hristova K The extracellular domain of fibroblast growth factor receptor 3 inhibits ligand-independent dimerization. Science Signaling 3, ra86 (2010). [PubMed: 21119106]
68. King C, Stoneman M, Raicu V & Hristova K Fully quantified spectral imaging reveals in vivo membrane protein interactions. Integr.Biol.(Camb.) 8, 216–229 (2016). [PubMed: 26787445]
69. Kim DH et al. Direct visualization of single-molecule membrane protein interactions in living cells. PLoS Biol 16, e2006660 (2018). [PubMed: 30543635]
70. Singh DR, King C, Salotto M & Hristova K Revisiting a controversy: The effect of EGF on EGFR dimer stability. Biochim Biophys Acta Biomembr (2019).
71. Macdonald JL & Pike LJ Heterogeneity in EGF-binding affinities arises from negative cooperativity in an aggregating system. Proceedings of the National Academy of Sciences of the United States of America 105, 112–117 (2008). [PubMed: 18165319]
72. Needham SR et al. EGFR oligomerization organizes kinase-active dimers into competent signalling platforms. Nat Commun 7, 13307 (2016). [PubMed: 27796308]
73. Huang Y et al. Molecular basis for multimerization in the activation of the epidermal growth factor receptor. Elife 5 (2016).
74. Ivanisevic L, Zheng W, Woo SB, Neet KE & Saragovi HU TrkA receptor “hot spots” for binding of NT-3 as a heterologous ligand. Journal of Biological Chemistry 282, 16754–16763 (2007). [PubMed: 17439940]

75. Meakin SO & Shooter EM The nerve growth factor family of receptors. Trends in neurosciences 15, 323–331 (1992). [PubMed: 1382329]
76. Zhang XQ et al. Receptor specificity of the fibroblast growth factor family - The complete mammalian FGF family. Journal of Biological Chemistry 281, 15694–15700 (2006). [PubMed: 16597617]
77. Murai KK & Pasquale EB 'Eph'ective signaling: forward, reverse and crosstalk. Journal of Cell Science 116, 2823–2832 (2003). [PubMed: 12808016]
78. Barquilla A & Pasquale EB Eph receptors and ephrins: therapeutic opportunities. Annu.Rev.Pharmacol.Toxicol. 55, 465–487 (2015). [PubMed: 25292427]
79. Stoneman MR et al. A general method to quantify ligand-driven oligomerization from fluorescence-based images. Nat Methods 16, 493–496 (2019). [PubMed: 31110281]
80. Valley CC, Lewis AK & Sachs JN Piecing it together: Unraveling the elusive structure-function relationship in single-pass membrane receptors. Biochim Biophys Acta Biomembr 1859, 1398–1416, d (2017). [PubMed: 28089689]
81. Bocharov EV, Sharonov GV, Bocharova OV & Pavlov KV Conformational transitions and interactions underlying the function of membrane embedded receptor protein kinases. Biochim Biophys Acta Biomembr 1859, 1417–1429 (2017). [PubMed: 28131853]
82. Bell CA et al. Rotational coupling of the transmembrane and kinase domains of the Neu receptor tyrosine kinase. Molecular Biology of the Cell 11, 3589–3599 (2000). [PubMed: 11029057]
83. Bocharov EV et al. Helix-helix interactions in membrane domains of bitopic proteins: Specificity and role of lipid environment. Biochim Biophys Acta Biomembr 1859, 561–576 (2017). [PubMed: 27884807]
84. Lu C et al. Structural evidence for loose linkage between ligand binding and kinase activation in the epidermal growth factor receptor. Mol Cell Biol 30, 5432–5443 (2010). [PubMed: 20837704]
85. Lu C, Mi LZ, Schurpf T, Walz T & Springer TA Mechanisms for kinase-mediated dimerization of the epidermal growth factor receptor. J Biol Chem 287, 38244–38253 (2012). [PubMed: 22988250]
86. Sabet O et al. Ubiquitination switches EphA2 vesicular traffic from a continuous safeguard to a finite signalling mode. Nat Commun 6, 8047 (2015). [PubMed: 26292967]
87. Sarabipour S & Hristova K Pathogenic Cysteine Removal Mutations in FGFR Extracellular Domains Stabilize Receptor Dimers and Perturb the TM Dimer Structure. J Mol Biol 428, 3903–3910 (2016). [PubMed: 27596331]
88. Needham SR et al. Measuring EGFR separations on cells with ~10 nm resolution via fluorophore localization imaging with photobleaching. PLoS One 8, e62331 (2013). [PubMed: 23650512]
89. Needham SR et al. EGFR oligomerization organizes kinase-active dimers into competent signalling platforms. Nat Commun 7 (2016).
90. Park Y et al. Single-Molecule Rotation for EGFR Conformational Dynamics in Live Cells. J Am Chem Soc 140, 15161–15165 (2018). [PubMed: 30380855]
91. Fleishman SJ, Schlessinger J & Ben Tal N A putative molecular-activation switch in the transmembrane domain of erbB2. Proc.Natl.Acad.Sci.U.S.A 99, 15937–15940 (2002). [PubMed: 12461170]
92. Bocharov EV et al. Structural basis of the signal transduction via transmembrane domain of the human growth hormone receptor. Biochim Biophys Acta Gen Subj 1862, 1410–1420 (2018). [PubMed: 29571748]
93. Bocharov EV et al. Structural Aspects of Transmembrane Domain Interactions of Receptor Tyrosine Kinases. Biophysical Journal, Supplement 100, 207a-1131-Pos (2011).
94. Bocharov EV et al. Structure of FGFR3 Transmembrane Domain Dimer: Implications for Signaling and Human Pathologies. Structure 21, 2087–2093 (2013). [PubMed: 24120763]
95. Keppel TR et al. Biophysical Evidence for Intrinsic Disorder in the C-terminal Tails of the Epidermal Growth Factor Receptor (EGFR) and HER3 Receptor Tyrosine Kinases. J Biol Chem 292, 597–610 (2017). [PubMed: 27872189]

Highlights

- We discuss the transition model of receptor tyrosine kinase activation.
- The model is grounded in the principles of physical chemistry.
- The model provides a framework to understand RTK activity and to make predictions.
- The model can empower the search for modulators of RTK function.

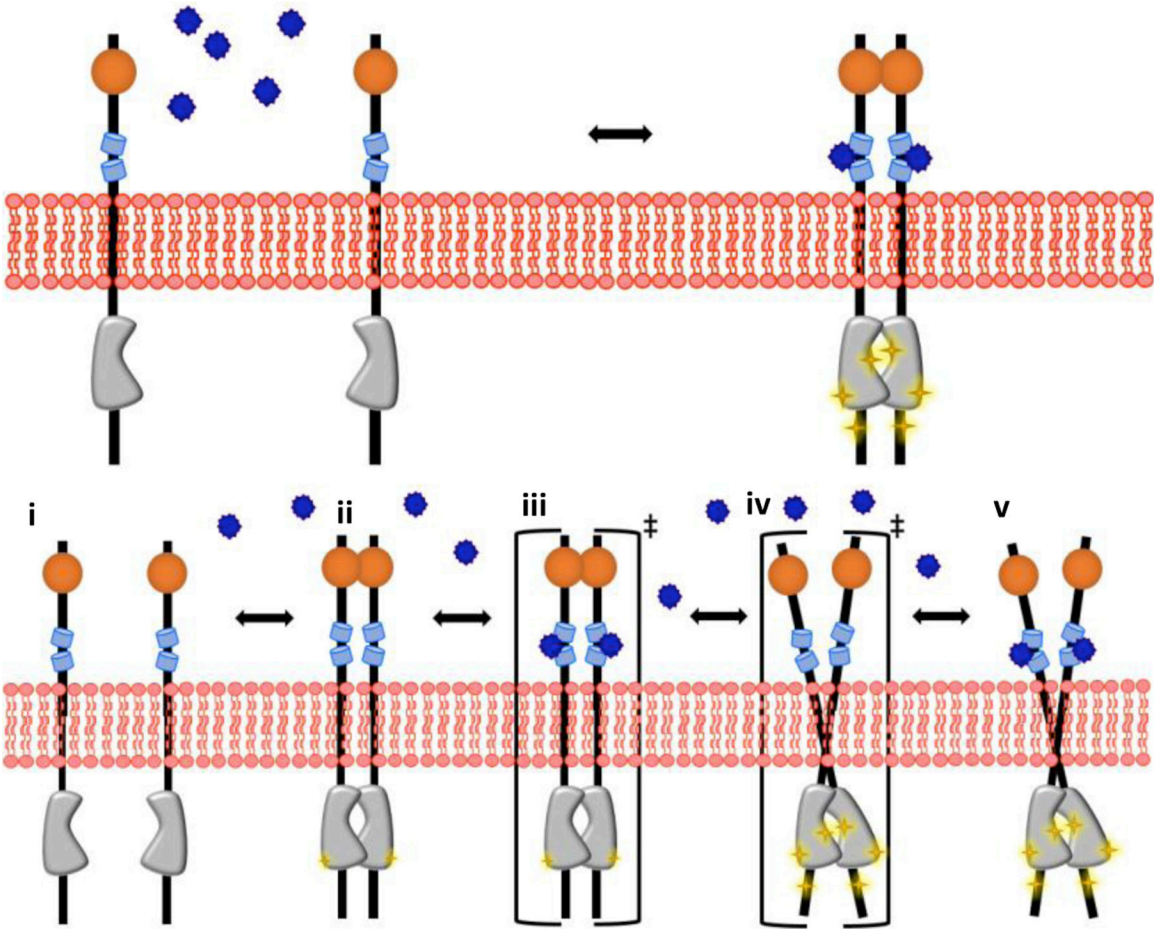

Fig. 1.

Receptor tyrosine kinases are single-pass membrane proteins which are activated after they associate in the plasma membrane. The canonical model (top) assumes that RTKs are monomeric and inactive in the absence of ligand (left) and become activated once the ligand binds and drives their dimerization (right). However, recent work has shown that RTK activation is much more complex. The transition model (bottom), which accounts for all possible states of the receptor, can be described via thermodynamic cycles (see Figures 3 and 4). It assumes that RTKs exist in an equilibrium between monomers (i) and dimers in the absence of ligand. The dimer can exist in an inactive (ii) or active confirmation (v). Ligand binding stabilizes the active dimer confirmation. A liganded, inactive dimer and an unliganded, active dimer (iii and iv) can also exist, although these are assumed to be low population transition states. Liganded monomers and singly liganded dimers (not shown) can also exist.

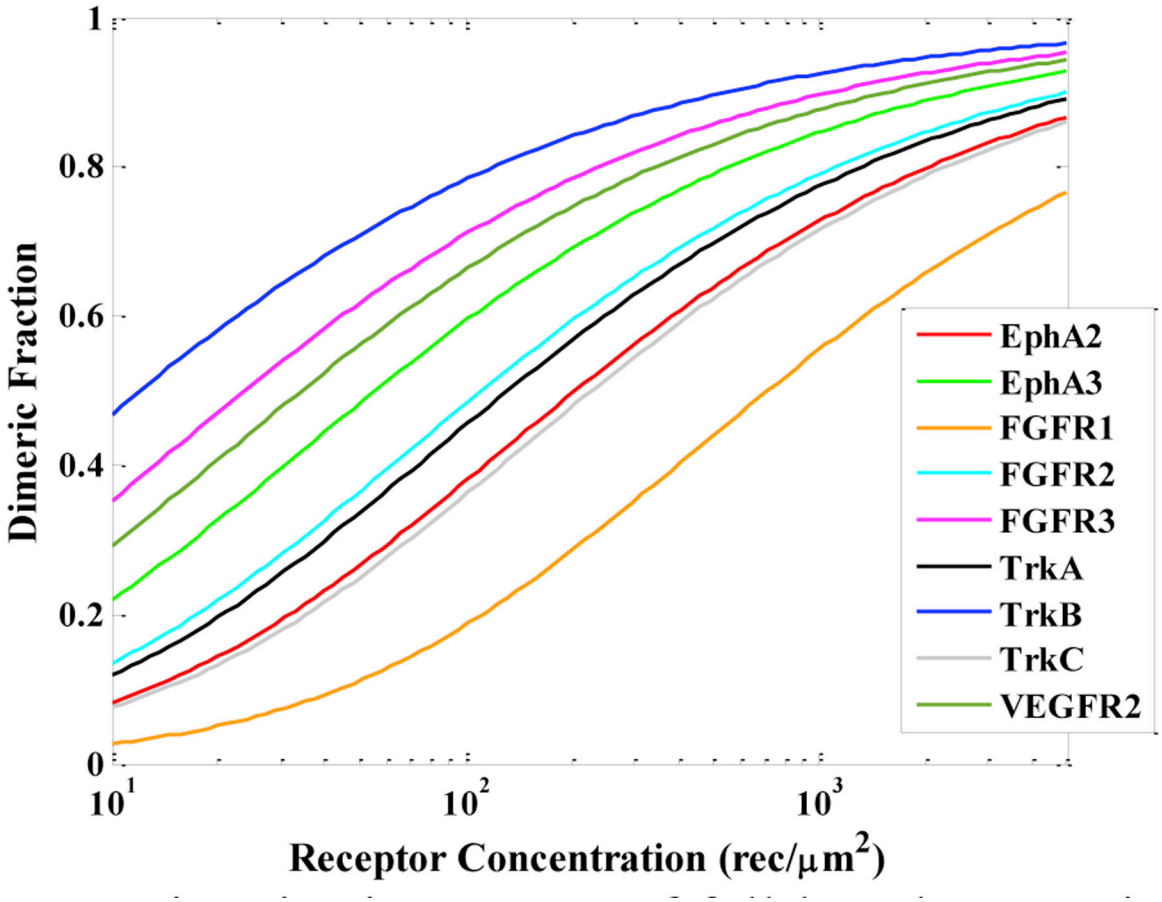

Fig. 2.

Dimerization curves of full-length RTKs in the absence of ligand. These curves are based on FRET measurements of interactions in mammalian membranes. The RTKs depicted and their corresponding K_{diss}'s (rec/μm^2) are EphA2 206 (red)[1], EphA3 55 (light green)[2,3], FGFR1 710 (orange)[10], FGFR2 11 (cyan)[10], FGFR3 24 (magenta)[10], TrkA 132 (black)[17], TrkB 12 (blue)[17], TrkC 227 (gray)[17,18], and VEGFR2 34 (dark green)[4,13,19].

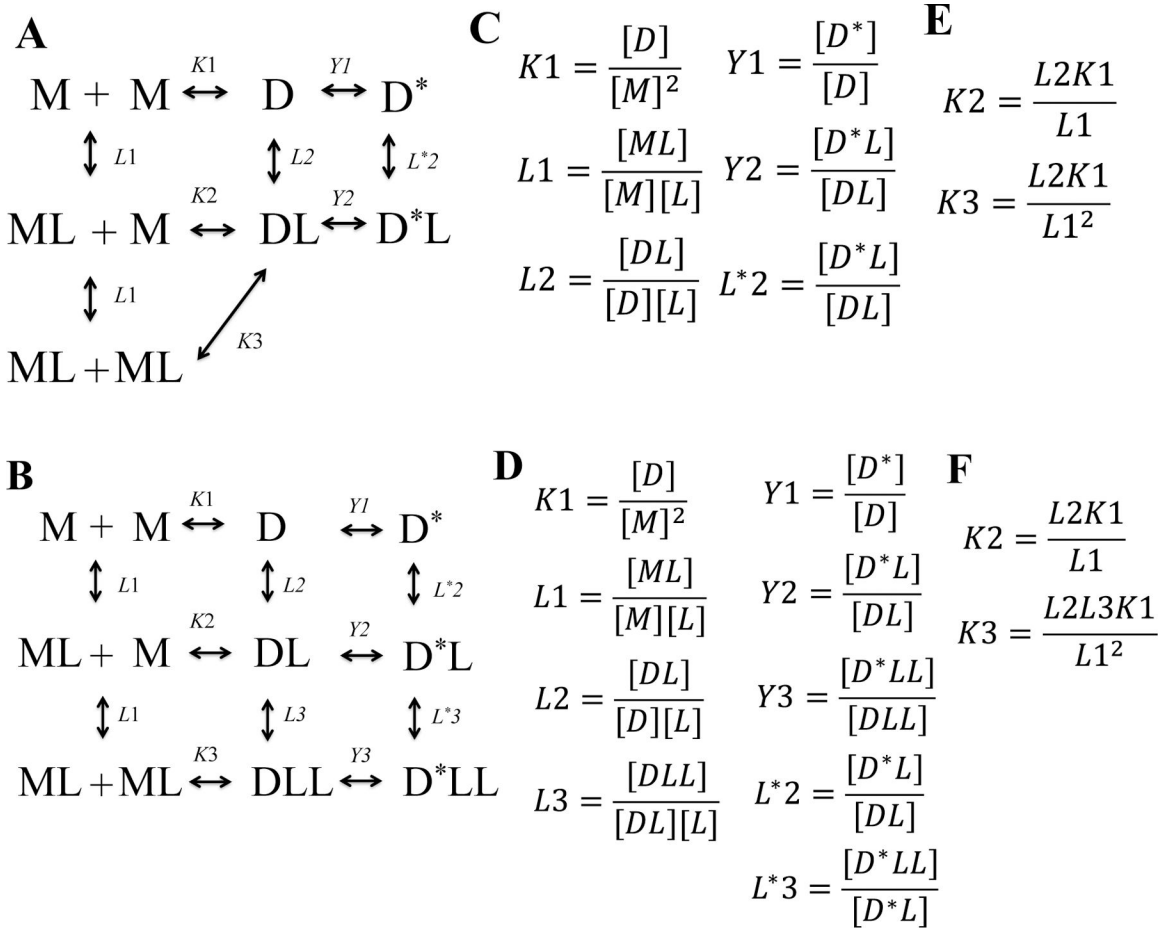

Fig. 3.

Thermodynamic cycles which embody the transition model of RTK activation. The dimerization constants in the cycles are denoted as *K*'s, and the ligand-binding constants are denoted as *L*'s. The *Y* constants denote possible allosteric transitions in the dimers. D* denotes an active dimer that has undergone this allosteric transition. (A) The process of RTK activation by a dimeric ligand. (B) The process of RTK activation by a monomeric ligand. (C) and (D) The definition of the association constants for the cycles shown in (A) and (B), respectively. (D) and (F) The links between association constants for the cycles shown in (A) and (B), respectively. Based on the current understanding of RTK activation, it is assumed that *Y1* is small (the unliganded dimers are not likely to adopt an active configuration), while *Y2* and *Y3* are large (the ligand-bound dimers have a strong preference for the activated configuration). Thus, the cycles reduce to the ones in Figure 4.

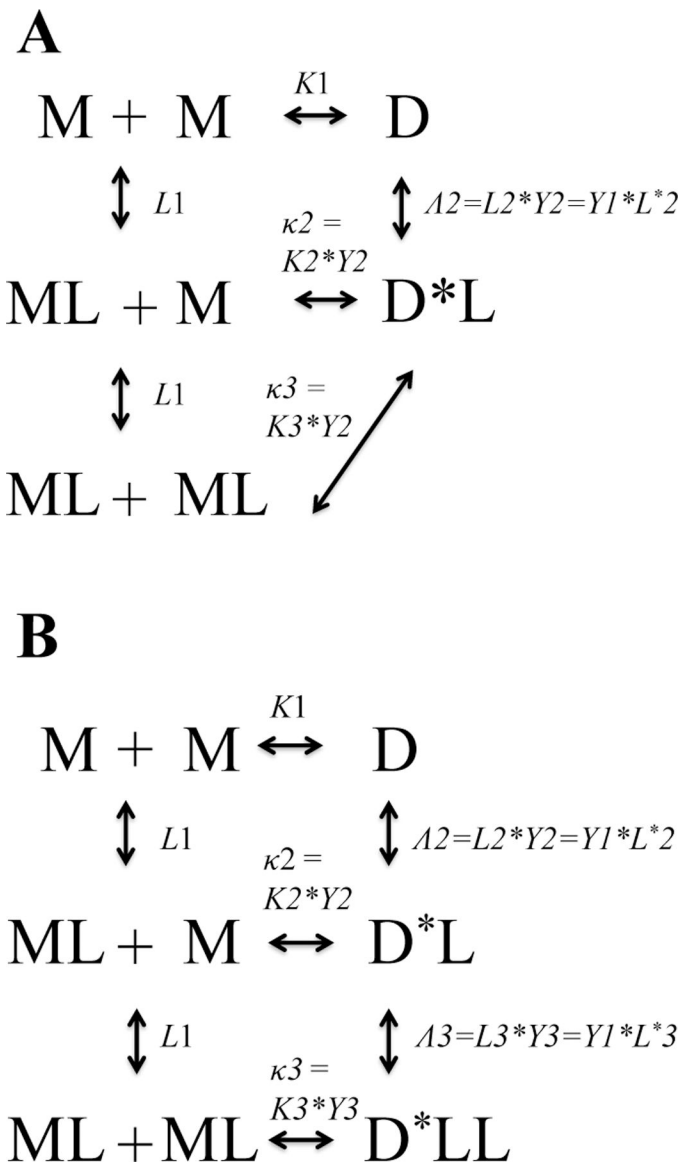

Fig. 4.

Working models that can be used to fit binding measurements. *D** denotes the active dimers. The binding constant Λ describes allosteric binding, and the binding constant κ describes allosteric dimerization. Λ is the product of the binding and allosteric constants, and κ is the product of the dimerization and allosteric constants. (A) The process of RTK activation by a dimeric ligand. (B) The process of RTK activation by a monomeric ligand.

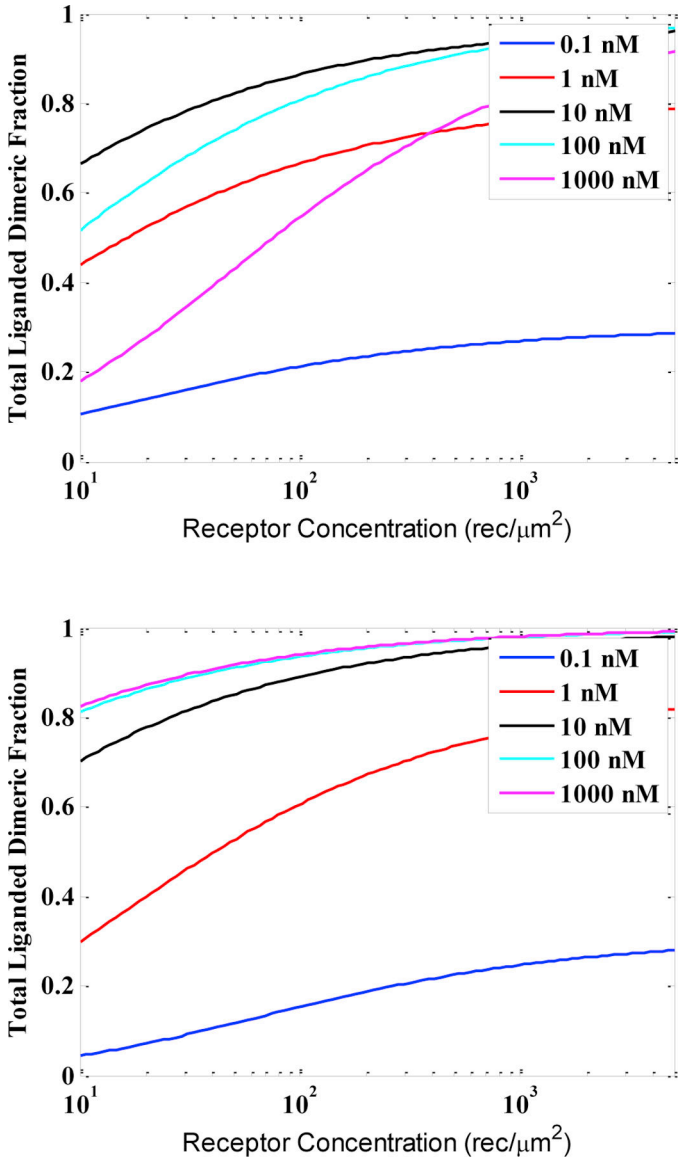

Fig. 5.

Predictions of liganded dimeric fractions as a function of receptor concentration for different fixed ligand concentrations. This is the active receptor fraction in the context of the working model in Figure 4. Top: Dimeric ligand (see Figure 4A for thermodynamic cycle) where $K1$ = .029 μm^2/rec, $L1 = 9.6*10^7$ M^{-1}, and $\Lambda 2 = 4.3*10^9$ M^{-1}. Bottom: Monomeric ligand (see Figure 4B for thermodynamic cycle) where $K1$ = .088 μm^2/rec, $L1 = 9.6*10^7$ M^{-1}, $\Lambda 2 = 4.3*10^9$ M^{-1}, and $\Lambda 3 = 4.3*10^8$ M^{-1}.

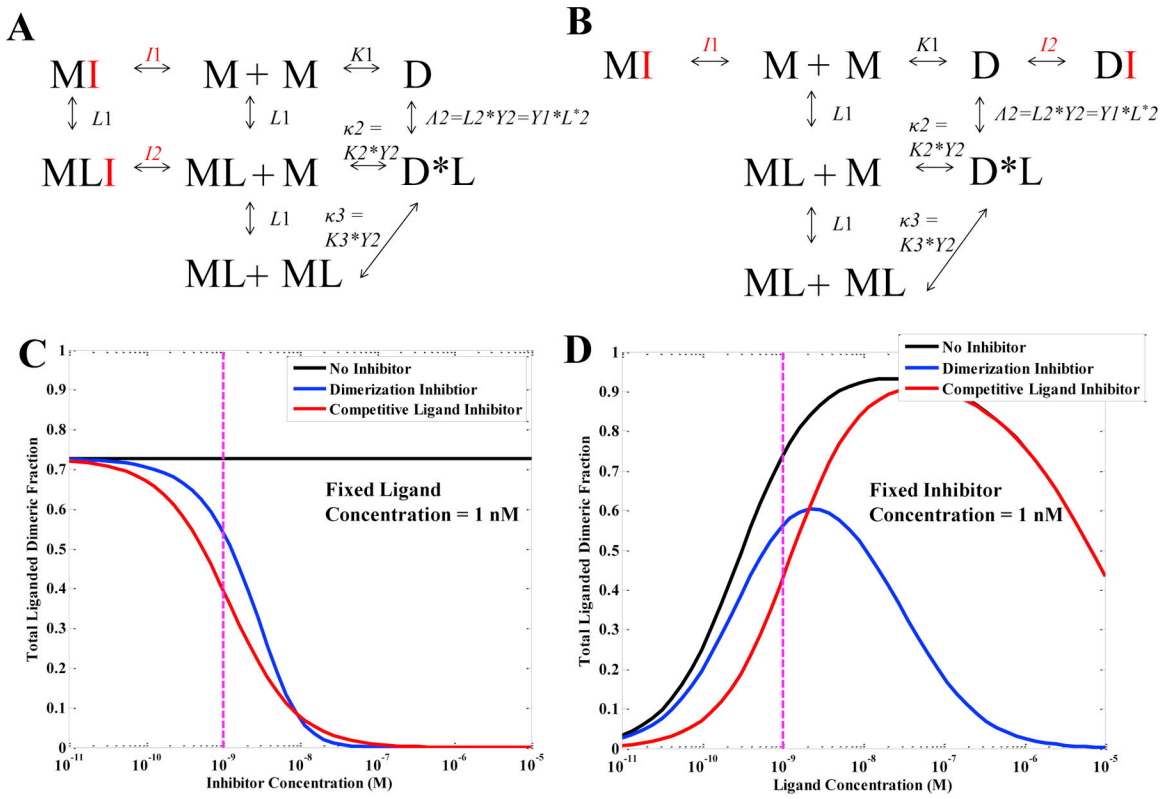

Fig. 6.

The transition model can predict the action of pharmacological modulators. (A) A thermodynamic cycle for a dimeric ligand (see Fig. 4A) and an inhibitor which blocks dimerization, but does not directly interfere with ligand binding. This inhibitor is assumed to bind to the dimerization interface and thus prevent receptor dimerization; it only binds to unliganded monomers (M) and liganded monomer (ML). (B) A thermodynamic cycle for a dimeric ligand and an inhibitor which competes with ligand binding, but does not directly interfere with dimerization. This inhibitor is assumed to bind to the ligand binding interface and thus prevent ligand binding; it only binds to unliganded monomers (M) and dimers (D). (C) & (D) Predictions of the effect of the two different inhibitors on theliganded dimeric fraction. The black curve is the case of no inhibitor, and the blue and red curves correspond to (A) and (B), respectively. (C) The liganded dimeric fraction as a function of inhibitor concentration, where the ligand concentration is 1 nM; the dashed magenta line indicates an inhibitor concentration of 1 nM. (D) The liganded dimeric fraction as a function of ligand concentration, where the inhibitor concentration is 1 nM; the dashed magenta line indicates a ligand concentration of 1 nM. In all cases, receptor concentration is 500 rec/μm^2, $K1$ = . 029 μm^2/rec, $L1$ = 9.6*10^7 M^{-1}, and $\Lambda 2$ = 4.3*10^9 M^{-1}; for the blue curve, $I1$ = $I2$ = 1.5*10^9 M^{-1} and for the red curve, $I1$ = 9.6*10^7 M^{-1} and $I2$ = 4.3*10^9 M^{-1}.